ELSEVIER

Journal of Neuroscience Methods 160 (2007) 75–84

JOURNAL OF NEUROSCIENCE METHODS

www.elsevier.com/locate/jneumeth

Using double-magnetic induction to measure head-unrestrained gaze shifts I. Theory and validation

Peter Bremen, Robert F. Van der Willigen, A. John Van Opstal *

Department of Biophysics, Institute of Neuroscience, Radboud University Nijmegen, Geert Grooteplein 21, 6525 EZ Nijmegen, The Netherlands

Received 2 May 2006; received in revised form 23 August 2006; accepted 24 August 2006

Abstract

So far, the double-magnetic induction (DMI) method has been successfully applied to record eye movements from head-restrained humans, monkeys and cats. An advantage of the DMI method, compared to the more widely used scleral search coil technique, is the absence of vulnerable lead wires on the eye. A disadvantage, however, is that the relationship between the eye-in-head orientation and the secondary induction signal is highly non-linear and non-monotonic. This limits the effective measuring range to maximum eye orientations of about ±30°.

Here, we analyze and test two extensions required to record the full eye-head orienting range, well exceeding 90° from straight-ahead in all directions. (1) The use of mutually perpendicular magnetic fields allows for the disambiguation of the non-monotonic signal from the ring. (2) The application of an artificial neural network for offline calibration of the signals. The theoretical predictions are tested for horizontal rotations with a gimbal system. Our results show that the method is a promising alternative to the search coil technique.

Keywords: Eye movements; Head movements; Double-magnetic induction; Search coil; Calibration

1. Introduction

Currently, two invasive electromagnetic methods for monitoring eye movements are being used in oculomotor research: the scleral search coil (SSC) technique, and the double-magnetic induction (DMI) method. The SSC technique has become the gold standard because: (1) it allows for high spatial (down to a few minutes of arc) and high temporal (typically 1 ms, or better) resolution, (2) it is approximately linear across the entire human (monkey and cat) oculomotor range (±40°), (3) it does not limit the field of view, (4) it can be applied in complete darkness, and even with closed eye lids, and (5) it can be readily used to measure head-free gaze shifts over the full motor range. To measure eye movements with the SSC technique in human subjects, a silicon annulus is placed on the eye (Collewijn et al., 1975; Robinson, 1963). This annulus contains an embedded coil made of thin copper wire with protruding lead wires connected to a detection device. When a subject is placed in the center of a periodically changing uniform magnetic field, eye orientation in space (gaze) can be determined from the amplitude of the induction voltage in the SSC.

The SSC method, however, has a number of drawbacks mostly linked to the lead wires (Bos et al., 1988; Bour et al., 1984; Malpeli, 1998). (1) Dragging of the wires through the eyelashes causes irritation, which limits experimental time to about 30 min. (2) Visual acuity deteriorates in the course of the experiment. (3) Breakage of the wires can occur during the experiments. (4) The lead wires, combined with the visco-elastic coupling between the SSC and the conjunctiva, have been hypothesized to introduce extra variability in eye movement kinematics, which is not observed with non-invasive, video-based eye-tracking methods (Smeets and Hooge, 2003; Van der Geest and Frens, 2001; see, however, Houben et al., 2006). These complications become increasingly significant when SSCs are implanted chronically in laboratory animals. There, the SSC is implanted beneath the conjunctiva. A small loop of wire is fashioned to give enough lead way for the eye to move. The connecting wire is then led subcutaneously up to the top of the head, where it is embedded in dental cement (Judge et al., 1979). The exit point of the wire introduces an additional risk for infections. However, the most important drawback, of the SSC technique is the considerable risk of wire breakage, making re-implantation of a new coil inevitable.

Abbreviations: DMI, double-magnetic induction; SSC, scleral search coil; 1D, one-dimensional

* Corresponding author. Tel.: +31 243 614 251.
E-mail address: j.vanopstal@science.ru.nl (A.J. Van Opstal).

0165-0270/$ – see front matter © 2006 Elsevier B.V. All rights reserved.
doi:10.1016/j.jneumeth.2006.08.012

The lead wire complications of the SSC method have prompted efforts to develop the so-called double-magnetic induction (DMI) method (Allik et al., 1981; Bos et al., 1988; Bour et al., 1984; Malpeli, 1998; Reulen and Bakker, 1982). In this method, the SSC is replaced by a short-circuited metal ring that is comparable in size to a SSC. Apart from prolonging experimental time in human subjects this also improves the comfort, as the need of connecting wires between the eye and recording equipment is avoided altogether. The head-restrained subject is seated in an alternating magnetic field that induces a current in the eye ring. The current strength depends on the orientation of the eye with respect to the magnetic field. This current, in turn, generates an additional secondary magnetic field that is picked up by a coil placed in close proximity to the ring and that remains stationary relative to the head. The secondary induction voltage in this, so-called, pickup coil depends on the current strength, and on the precise geometrical relationship between pickup coil and ring. Because the signal in the pickup coil also contains a contribution from the primary magnetic field, an additional coil, the so-called compensation coil is placed in the magnetic field and connected in anti-phase with the pickup coil. The primary component can thus be subtracted from the pickup coil's signal, and what remains, is the contribution of the ring.

Apart from requiring a head-restrained subject, the main drawback of the DMI method, however, is that the effective measurement range is limited to about 30°, due to complicated geometrical relationships and a non-monotonic, non-linear dependency between eye orientation and signal. The linear range, being only about ±10°, is even more restricted (Reulen and Bakker, 1982). To deal with this problem, Bour et al. (1984) proposed a calibration procedure that employed a quadratic polynomial fit of the data. Later, Bos et al. (1988) improved the description of the inherent non-linearity by using the electrodynamical concept of mutual induction that for a fixed geometrical relationship between ring and pickup coil was derived from the Biot-Savart law. So far, the DMI method has been used successfully in head-restrained humans (e.g. Reulen and Bakker, 1982), monkeys (e.g. Bour et al., 1984) and cats (Malpeli, 1998). The spatial and temporal resolution of the DMI method is comparable to that of the SSC. Still, the limited effective measurement range and the complex setup, together with the high susceptibility to noise due to insufficient compensation of the primary field, has so far restricted the design of experiments with human subjects. However, the major advantage of the DMI method, compared to the SSC technique, is the easy implantation of the ring in animal subjects and the lack of connecting wires, which not only makes re-implantations unnecessary but also minimizes the risk of infections.

In this study, we investigated how to overcome the inherent limitations of the DMI method so that it may be used in a greater variety of experimental setups. Our main aim is to use the DMI method in head-unrestrained subjects, and apply it over the full gaze-motor range, well exceeding 90° in all directions. To understand the basic underlying principles in this situation, we have extended the theoretical approach of Bos et al. (1988) to a head-unrestrained condition, and to a more realistic situation in practice, in which neither the ring/pickup coil assembly, nor the pickup coil and compensation coil system are perfectly aligned.

To test the theoretical predictions of our analysis, we employed a dummy platform to simulate the subjects' head and eye movements over the 180° left/right range from straight-ahead in the horizontal plane. To calibrate these data two extensions to the original DMI method (Bour et al., 1984; Malpeli, 1998; Reulen and Bakker, 1982) were made. (1) Three mutually perpendicular, primary magnetic fields were used instead of two, enabling for a disambiguation of the non-monotonic ring signal. (2) A model-free artificial neural network was employed to calibrate this signal. Our results indicate that the extended DMI method may be a promising alternative for the SSC technique.

2. Methods

2.1. Theoretical considerations for 1D eye rotations in the horizontal plane

2.1.1. Idealized situation

For the head-restrained situation, Bos et al. (1988) derived on the basis of mutual induction between the ring and the pickup coil and the Biot-Savart law that the voltage induced in the pickup coil by the ring is given by

$$V_h(\alpha, t) = K_h(t)\sin(\alpha)L[\cos(\alpha)] \quad (1)$$

with α the horizontal eye-in-head orientation, $K_h(t)$ is a proportionality constant that depends on the geometry of the system and the time-varying horizontal magnetic field strength, and $L[\cos(\alpha)]$ is a shape factor that expresses the geometrical non-linearity of the DMI method (see below).

Using the parameter notation introduced by Reulen and Bakker (1982) the coefficient $K_h(t)$, can be expressed as

$$K_h(t) = -N_{coil}N_{ring}\omega_h^2 B_h \sin(\omega_h t)\frac{\pi^2\mu_0 R_{ring}^3 R_{coil}}{bZ_{elec}} \quad (2)$$

with

$$b = \sqrt{(R_{eye}+d)^2 + R_{coil}^2} \quad (3)$$

In Eq. (2), N_{coil} and N_{ring} are the number of turns of the coil and the ring ($N_{ring} = 1$), respectively. ω_h and B_h are the angular frequency and strength of the horizontal primary magnetic field, respectively. Time is denoted as t, and μ_0 denotes the magnetic permeability. R_{coil}, R_{ring} and R_{eye} are the radii of the pickup coil, ring and eye, respectively. Z_{elec} is the electrical impedance of the ring and d in Eq. (3) denotes the coaxial distance between the ring and the pickup coil.

In Eq. (1), $\sin(\alpha)$ gives the strength of the magnetic flux through the ring (Fig. 1) as a function of horizontal eye rotation over azimuth angle α. Since in this case the head is fixed, α represents the angle of the ring with respect to the horizontal primary magnetic field, hereafter referred to as the horizontal field. Most notably, apart from the right-hand factor, $L[\cos(\alpha)]$, and details in the proportionality constant $K_h(t)$, V_h is identical as determined for the SSC technique (Collewijn et al., 1975; Robinson, 1963).

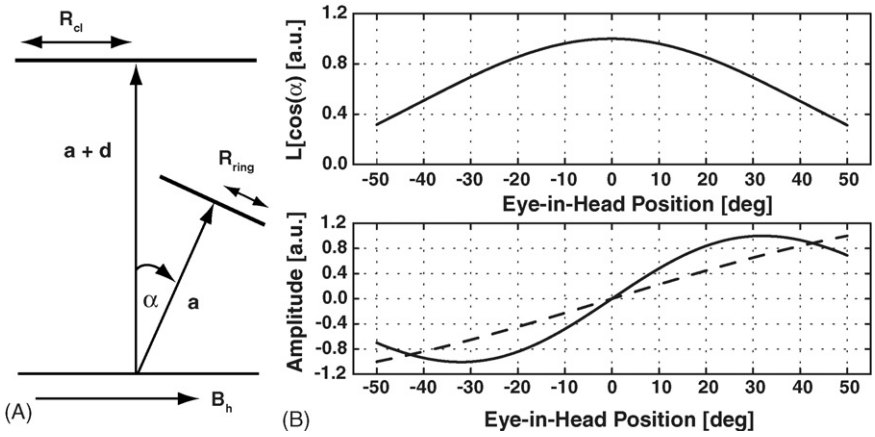

Fig. 1. (A) Geometry of the head-restrained DMI method, in which the pickup coil (radius R_{cl}, at a minimum distance d from the ring) is parallel to the magnetic field (B_h). Here, the eye (radius a) with the ring (radius R_{ring}) has been rotated by angle α with respect to the normal vectors of the coil and the field. The axes of coil and ring intersect at a common rotation center. We refer to this as the ring/pickup coil assembly. (B, top) The ring-coil shape factor $L[\cos(\alpha)]$ as function of the eye-in-head orientation (Eq. (2)). (B, bottom) The non-linear relation of the predicted signals in the pickup coil as function of α (Eq. (1); solid line) reaches a maximum near $\alpha = 30^\circ$ (for fixed $a = 1.2$ cm, $d = 2$ cm, $R_{ring} = 0.8$ cm, $R_{cl} = 2.5$ cm). The dashed line corresponds to the strength of the induction current in the ring (or to the signal as obtained from the traditional search coil method) and is proportional to $\sin(\alpha)$.

The shape factor $L[\cos(\alpha)]$ distinguishes the DMI method from the SSC technique by introducing an additional non-linearity that limits the measurement range between $\pm 30^\circ$. In particular, $L[\cos(\alpha)]$ expresses the geometric relationship between of the ring and the pickup coil by

$$L[\cos(\alpha)] = \sum_{n=1}^{\infty} \frac{1}{n(n+1)} \left(\frac{c}{b}\right)^n P_n^1 \left(\frac{R_{eye}}{c}\right) P_n^1 \left(\frac{R_{eye}+d}{b}\right) \times P_n(\cos(\alpha)) \quad (4)$$

with

$$c = \sqrt{R_{eye}^2 + R_{ring}^2} \quad (5)$$

Here, P_n are Legendre polynomials and P_n^1 are associated Legendre polynomials of the first kind. In practice, the first six polynomials ($n = 6$) suffice to adequately approximate this series to within 0.05% (Bos et al., 1988).

The DMI method can be readily extended to two dimensions, by adding a vertical primary magnetic field, with its own driving frequency, ω_v and magnetic field strength, B_v (Bos et al., 1988; Bour et al., 1984; Reulen and Bakker, 1982).

It should be noted that Eq. (1) is only valid for the idealized situation in which the axes of the ring and pickup coil are aligned, i.e. they intersect at the common origin of rotation (see Fig. 1A). A second approximation in Eq. (1) is that the primary magnetic field does not induce a net voltage in the pickup coil, i.e. the coil's orientation is exactly parallel to the magnetic field. In practice, these assumptions may not be exactly met, in which case Eqs. (1) and (2) will have to be modified. We will deal with this non-ideal situation in Section 2.1.2. First, we proceed with the idealized coaxial condition, and perfect primary field cancellation.

Fig. 1A shows the coaxial 1D situation, with B_h the horizontal field, and α the eye-in-head orientation. Fig. 1B (top) shows the geometrical factor $L[\cos(\alpha)]$ as function of α (Eq. (2), up to $n = 6$), together with the prediction of the pickup voltage according to Eq. (1) (bottom). As can be seen from Fig. 1B (bottom), although the current strength in the ring varies as $\sin(\alpha)$ (dotted line), which is nearly linear for angles within the oculomotor range (up to about $\pm 40^\circ$), the coil's secondary induction voltage depends in a highly non-linear way on the ring's orientation (solid line). A more severe problem with the DMI method, however, is its limited measurement range, as the signal reaches its extremes at about $\alpha = \pm 30^\circ$.

Therefore, in its present form the method is useless when eye orientations would exceed the $\pm 30^\circ$ to 35° range, because the secondary induction voltage then becomes ambiguous. For head-restrained conditions, however, this potential ambiguity is not problematic, since the available measurement range covers a major part of the human (cat and monkey) oculomotor range. Under natural conditions ocular excursions beyond 30° eccentricity are rare and can be readily constrained within an experiment. In head-unrestrained subjects, this is of course not feasible. We will address the issue of head-unrestrained gaze shifts in the following paragraphs.

Note, that in Eq. (1) the $L[\cos(\alpha)]$ term is only determined by the geometry of the coil-ring assembly, and does not depend on the orientation of that assembly with respect to the primary magnetic field. In contrast, the $\sin(\alpha)$ factor is only determined by the flux of the primary magnetic field through the ring. Therefore, in the situation that the entire assembly of Fig. 1A is rotated by angle γ with respect to the horizontal magnetic field (this simulates a head turn; see Fig. 2), only the $\sin(\alpha)$ term in Eq. (1) will change and V_h becomes

$$V_h(\alpha, \gamma, t) = K_h(t) \sin(\alpha + \gamma) L[\cos(\alpha)] \quad (6)$$

In Eq. (6), angle α is the orientation of the eye in the head, γ is the rotation of the head-in-space. Thus, their sum $\alpha + \gamma$ represents the direction of gaze (eye-in-space). The inherent non-linearity of the DMI method (due to $L[\cos(\alpha)]$, see Fig. 1B, top) is therefore not influenced by head-unrestrained gaze shifts.

Instead, for eye-in-head orientations in the 30–35° range the curve in Fig. 1B (bottom) will now shift as a function of head

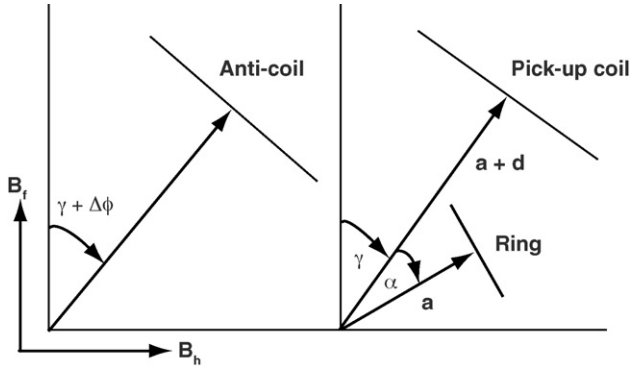

Fig. 2. Hypothetical DMI geometry for head-free gaze shifts. The anti-coil is positioned at a sufficiently large distance from the ring (e.g. on the head). Its electrical properties are identical to those of the pickup coil, but may make a small, fixed, angle $\Delta\phi$ with it. Angle α is the orientation of the ring relative to the pickup coil; γ is the angle of the pickup coil with respect to the magnetic field, B_h, and corresponds to the head orientation in space. Their sum, $\alpha+\gamma$, is the eye orientation in space (gaze). B_f is an additional frontal magnetic field.

orientation, as determined by the factor $\sin(\alpha+\gamma)$. Accordingly, the ambiguity of the eye-in-head signal will shift by the same amount, considerably restricting the monotonic measurement range in the direction of head rotation (Fig. 3, solid curves).

However, the introduction of an additional primary magnetic field that is perpendicular to the horizontal field, will fully resolve this ambiguity, and in addition, drastically improve the resolution of the system near the extremes. A frontal primary field, with strength B_f and frequency ω_f, induces the following secondary voltage in the pickup coil:

$$V_f(\alpha,\gamma,t) = K_f(t)\cos(\alpha+\gamma)L[\cos(\alpha)] \quad (7)$$

Eq. (7) is identical to Eq. (6) except that $\sin(\alpha+\gamma)$ now becomes $\cos(\alpha+\gamma)$.

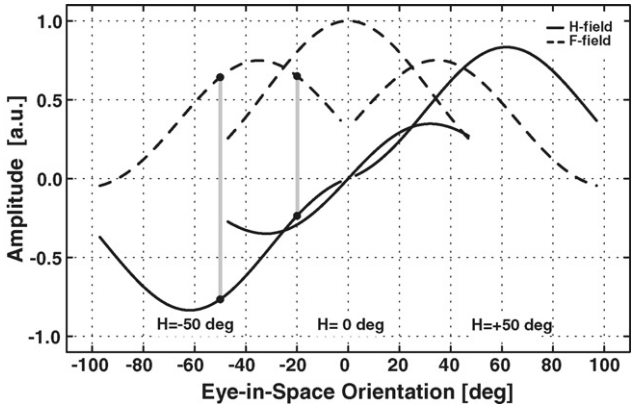

Fig. 3. Predicted pickup coil signals for the horizontal (solid line, H-field) and frontal fields (dashed line, F-field) as function of the eye-in-space orientation, shown for three different head orientations (50° leftward, straight-ahead, and 50° rightward) assuming an ideal geometry as depicted in Fig. 2. The eye-in-head orientation is restricted to ±45°. Note that, the shape of the DMI non-linearity varies with the head orientation (see Eq. (6)). Because the voltages induced by the two magnetic fields have a 90° phase difference, a peak or valley in one field's signal coincides with a monotonic relation for the other field (e.g. between the points connected by the gray vertical lines). Thus, even though the signal from the horizontal field may be ambiguous, the eye-in-head orientation can be uniquely retrieved, once the head-in-space orientation is known.

In Fig. 3, simulated signals of the frontal induction voltages for three head orientations (straight-ahead, and ±50° horizontal) are plotted as function of gaze (with the eye-in-head orientation $-45° < \alpha < +45°$; dashed lines), for the idealized situation that the primary signals in the anti-coil and pickup coil fully cancel. With the help of Eq. (7) it is possible to disambiguate the non-monotonic input-output relation of the ring/pickup coil assembly as will be discussed in Section 2.1.2. Note here, however, that for each head orientation a unique combination of voltages for the horizontal (H-field) and frontal (F-field) fields exists, as indicated by the black dots connected by the gray vertical lines. As an example, the signal of the frontal field for 50° and 20° eye orientation is ambiguous as indicated by the black dots. Nevertheless, the signals for the same eye orientations of the horizontal field are not ambiguous (black dots). In combination with the head orientation there will always be a unique combination of signals that exactly determines the eye-in-head orientation.

Finally, it is important to note, that Eqs. (6) and (7) assume that the primary induction voltage in the pickup coil is fully cancelled by a compensation coil (see Fig. 2, anti-coil). For this to work, however, the two coils need to be identical in their electrical properties, the compensation coil should not be influenced by the ring, should be exactly parallel to the pickup coil, and the magnetic field should be perfectly homogeneous. In practice, however, even though the coils may be identical, minor inhomogeneities of the field will be present, and the two coils will not be exactly aligned. Below, we will deal with this situation.

2.1.2. Non-idealized situation

In case of imperfect cancellation, there will be an additional net primary field voltage in the pickup coil's signal. Theoretically this voltage would be determined by the geometrical difference of the two otherwise identical coils and would depend only on the head orientation, γ. As noted in Eq. (8) for the horizontal field:

$$V_{net,h}(\gamma,t) = L_{cl,h}\sin(\omega_h t)[\sin(\gamma) - \sin(\gamma+\Delta\phi)] \quad (8)$$

with $L_{cl,h}$ a constant, proportional to the coils' self-induction (here taken to be identical for the two coils), and $\Delta\phi$, the (small) difference in angle between the coils and the magnetic field lines (Fig. 2). In practice, however, the electrical and geometrical properties of the two coils will not be identical, rendering the dependency of the net voltage on head movement slightly more complicated (e.g. Fig. 8C and D). A quantitative description of the exact relation, however, is not necessary for the calibration of the signals. Since (1) it is possible to measure V_{net} before the experiment (humans: measurement without ring; animals: coils are usually fixed to an assembly that can be measured without the animal). V_{net} can then be subtracted from the experimental data offline. (2) In the neuronal network calibration approach the network will not be hampered by a complex V_{net} function, since the unique relationship between the secondary induction voltages and gaze remains unchanged as is explained below.

Since perfect cancellation for all head orientations is not attainable in practice, the induction voltages measured by the

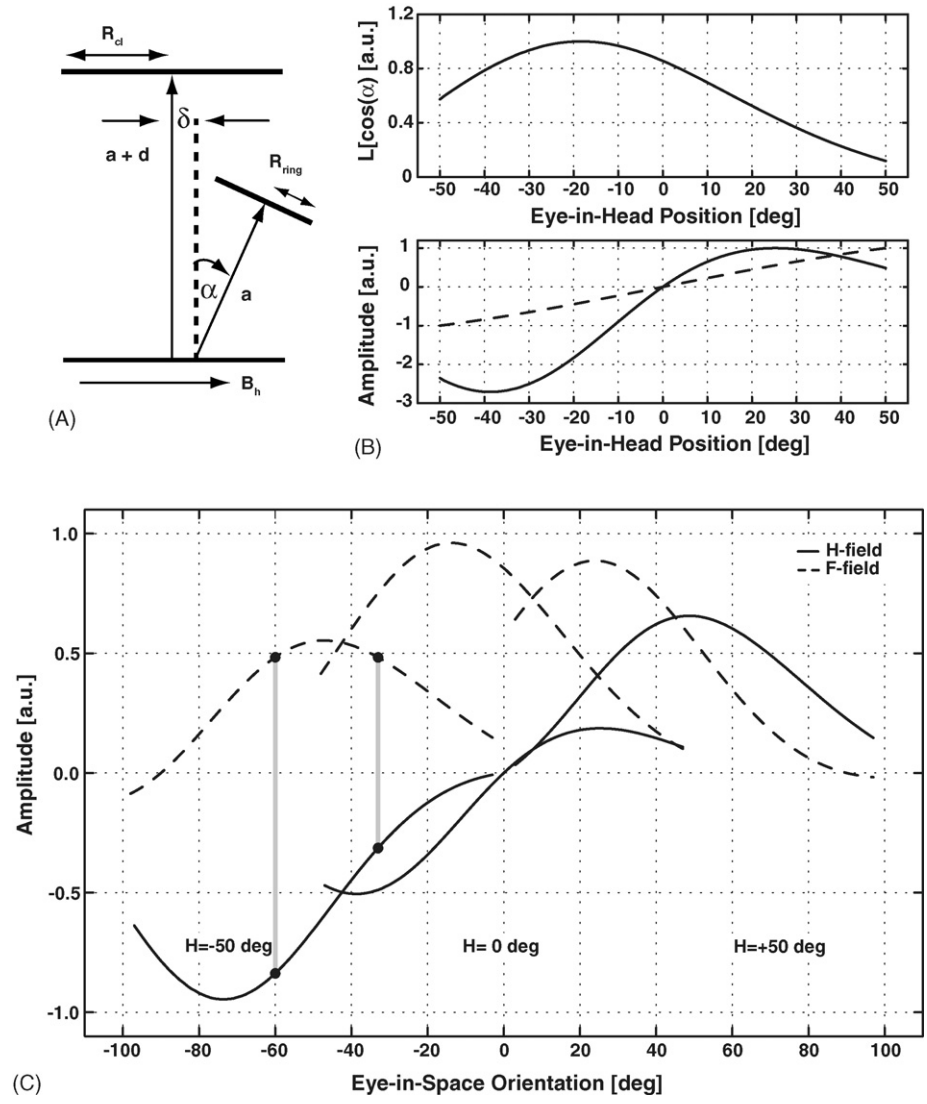

Fig. 4. Simulation of a condition in which the axes of ring and pickup coil are not collinear, instead the ring's center is moved by $\delta = 0.8$ cm toward the right relative to the pickup coil's center (A). This misalignment causes the geometrical non-linearity to become asymmetric relative to $\alpha = 0^\circ$ (B, top). The monotonic measurement range has shifted towards the left, at the expense of a smaller range to the right (B, bottom). Nevertheless, together with the frontal field, the eye-in-head position can still be retrieved over the full oculomotor range (C, compare the points connected by the gray vertical lines).

pickup coil are described as

$$V_h(\alpha, \gamma, t) = K_h(t)\sin(\alpha + \gamma)L(\cos\alpha) + V_{net,h}(\gamma, t),$$
$$V_f(\alpha, \gamma, t) = K_f(t)\cos(\alpha + \gamma)L(\cos\alpha) + V_{net,f}(\gamma, t) \quad (9)$$

Thus, imperfect cancellation of the primary field contributions in the pickup coil will merely add an offset to the signals that varies as a function of the head orientation, without affecting the shape of the signals.

It is also to be expected that the assumption of a perfectly aligned ring/pickup coil assembly is violated in practice. That is, the rotation axes of the ring and the pickup coil will often not coincide (Fig. 4A). For example their axes may be shifted with respect to each other (δ, Fig. 4A). This shift will remain constant for all eye orientations (the ring on the eye rotates about angle α, Fig. 4A). It is then important to realize that this will only affect the $L[\cos(\alpha)]$ term in Eqs. (1), (6), (7) and (9), but not the induction current in the ring, and the primary induction voltages in the coils.

Yet, in general the analytical solution of this problem is not straight forward, and has to be done by numerical approximations of the Biot-Savart law. Our calculations show that the main effect, of such a misalignment is the introduction of an asymmetry in the shape factor $L[\cos(\alpha)]$, with respect to the straight-ahead eye-in-head fixation direction ($\alpha = 0^\circ$). In other words, the peak of this function will shift leftward when the ring's axis is shifted to the right, or rightward when it is shifted to the left of the center of the pickup coil. As a result, the shape factor $L[\cos(\alpha)]$ can no longer be described analytically by simple Legendre polynomials. Fig. 4B (top) shows the result of a numerical simulation of this effect when the ring was shifted rightward with respect to the coil's center by a full radius $\delta = 0.8$ cm. As a result, the linear range of the pickup coil signal has shifted to the left and ambiguity in the signal already arises for relatively

small positive angles of eye orientation (Fig. 4B, bottom). This can be seen in greater detail in Fig. 4C. Although an asymmetry of the signals as function of eye-in-head orientation is now apparent, frontal and horizontal field signals still form unique combinations as function of the gaze angle over the full range (Fig. 4C, black dots connected by vertical gray lines). Thus, the combination of head orientation γ, V_h and V_f constitutes a triplet of values that uniquely defines the eye orientation in the head.

2.2. Practical application

So far, we have extended the theoretical analysis of the DMI method by Bos et al. (1988) to head-unrestrained gaze shifts. In what follows, we describe an experimental test of the method on a gimbal system. We also propose a non-parametric calibration procedure that relies on a feed forward neural network to reconstruct the eye-in-head orientation, α, from the signals measured by the pickup coil and anti-coil over a large $\pm 120^\circ$ range of gaze shifts from the straight-ahead direction.

2.2.1. Test on a gimbal system

A custom-made gimbal system was used to simulate combined eye/head movements in the horizontal plane. This system consisted of a horizontal plateau that could manually be rotated about a vertical axis to simulate horizontal head rotations over the full 360° range. Two coils were mounted on the plateau inside two Fick gimbals (e.g. Crawford et al., 1999) that allowed independent alignment of the coils both horizontally and vertically with respect to the magnetic fields, and to each other (Fig. 5).

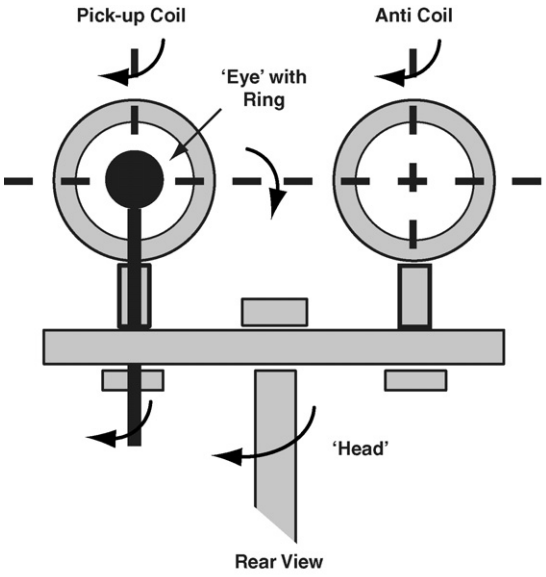

Fig. 5. Gimbal system used to test the head-unrestrained DMI method. The pickup coil with a ring on an artificial globe placed behind it (left) and the anti-coil (right) are each mounted inside a Fick gimbal on top of a horizontal plateau that can be rotated around a vertical axis. In this way the 'eye' and 'head' can be rotated independently in the horizontal plane, and the two coils can be optimally aligned with respect to the fields and each other. The distance of 1.8 cm of the ring relative to the pickup coil, as well as, the size (diameter 5 cm) of the pickup coil itself was chosen to mimic the situation attainable in subjects. Notice also that the absolute position of the ring on the artificial globe determines δ of Fig. 1.

The anti-coil and pickup coil were connected in anti-phase, such as to produce cancellation of the primary magnetic fields. The whole system was positioned in the center of three orthogonal, square-wave pulsed magnetic fields consisting of three pairs of Helmholtz coils of 2.5 m × 2.5 m and a Remmel field-generating system (Remmel, 1984; EM 5 Remmel Labs., Katy, TX, USA; frontal field: 48 kHz, 25 mV rms at a gain of 50, horizontal field: 60 kHz, 25 mV rms at a gain of 50). The pickup coil and anti-coil consisted of 50 turns of 0.1 mm insulated wire, with a diameter of 5.0 cm, and had a self-induction of 0.3 mH, and a dc resistance of 17 Ω (Malpeli, 1998). The diameter was chosen such that it would not occlude the field of vision of a human subject. For animal subjects the diameter may be slightly smaller. The ring was made of gold-plated copper, shaped such that it would fit around the cornea of a human eye (Bour et al., 1984). It had a central diameter of 1.3 cm, and a width of 4 mm. It could be placed behind the pickup coil on an artificial globe, at several distances and positions with respect to the coil's center, and could be manually rotated about the vertical axis to simulate horizontal eye rotations in the head.

To minimize the primary field component, the two coils were manually aligned. The system (without the ring) was rotated in the horizontal plane, and the anti-coil's orientation was adjusted to produce a minimal peak amplitude. Due to minor inhomogeneities in the fields, and to small differences between the two coils, a full cancellation across the entire measurement range was not achieved. Typically, the peak amplitude of the difference signal (about 2.0 V at a gain of 300) was about twice the peak-to-peak amplitude of the secondary induction voltage generated by the ring.

Once the two coils were aligned, the ring was positioned in the assembly, at a fixed distance of 1.8 cm behind the center of the pickup coil. The offsets of the anti-coil and pickup/anti-coil differences from the horizontal field were set to zero for the condition in which the eye and the head were both facing the straight-ahead direction. Since the signal of the frontal field follows a cosine behavior (Eq. (7)), this field was zeroed at -90° relative to the horizontal field direction. Then, the following set of measurements was performed: for each head position, the eye was rotated between -45° and $+45^\circ$, in 5° steps. The gimbal system was rotated between $\pm 180^\circ$ in 10° steps; thus resulting in a total of $19 \times 36 = 684$ measurements.

The system was designed such that a large number of variable settings was possible. Here, we only concentrate on a setting that would typically resemble a recording from human or animal subjects. That is, a distance of 1.8 cm between ring and pickup coil and a radius of 2.5 cm for the pickup coil. In the case of human subjects a precisely fitting bite-board could be employed on which both pickup coil and anti-coil can be mounted. In animal subjects both coils can be mounted on implanted head posts. Note, however, that the anti-coil does not have to be placed in the immediate vicinity of the pickup coil, as long as the magnetic field is sufficiently homogeneous.

2.2.2. Calibration

The recorded coil difference voltages, V_h^D, and V_f^D, were calibrated by applying a three-layer feed forward neural

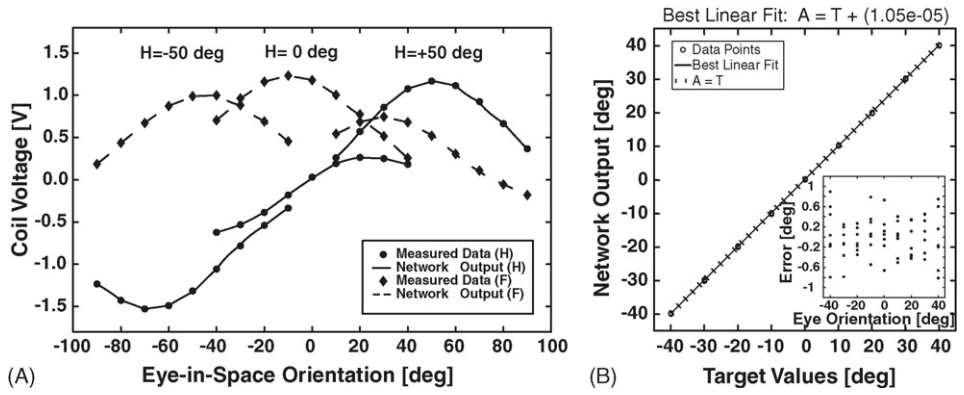

Fig. 6. (A) Measured voltages in the pickup coil for three different head-in-space orientations (−50°, 0°, +50°). The net primary signal has been subtracted. Eye-in-head positions range from −40° to +40° in steps of 10° for each head orientation. Circles denote signals from the horizontal field and diamonds from the frontal field. The calibrated network output is plotted as solid lines for the horizontal field and dashed lines for the frontal field, respectively. The network was trained on data limited to a head range of −90° to +90° in steps of 30° and an eye range from −40° to +40° in steps of 10° ($\sum$63). (B) Network output vs. target values for seven different head positions. Data is fitted with a linear function ($r^2 = 0.998$, $N = 63$). Inset: difference between network output and target values for each eye orientation at seven different head orientations.

network. The three input units of the network were: (1) V_h^D, (2) V_f^D, and (3) γ (as set on the gimbal system), while the desired, single output of the network was the eye-in-head angle, α. The network, which contained one layer of eight hidden units, was trained using the Bayesian-regularization implementation of the back-propagation algorithm (Matlab 7.0, Neural Networks Toolbox, The Mathworks Inc.) in order to avoid over-fitting (MacKay, 1992). The network was trained on a restricted subset of the sampled data: only 63 of the 684 recorded data points were used. These included head orientations from −90° to +90° in steps of 30° and eye orientations of −40° to +40° in steps of 10°. This set was designed to mimic a data set as would be typically obtained during an actual calibration session with a human subject. After training, the network's performance was tested on a set of interpolated values (interpolation factor 40), of which the training data were a subset.

3. Results

3.1. Calibration of the secondary induction signals

The recorded signals could be calibrated reliably. Fig. 6A shows the results of gimbal eye movement measurements and calibration for the same three head orientations as shown in Figs. 3 and 4. To achieve a better comparison with those two figures, V_{net} was subtracted. Note, however, that this subtraction is not necessary to achieve a good calibration. Markers denote data points (circles: horizontal field; diamonds: frontal field) and lines (solid: horizontal field; dashed: frontal filed) the network's output to the interpolated data set.

Note, that compared to the theoretical data of Fig. 3, the measured curves of Fig. 6 are shifted leftward; creating the predicted asymmetry as shown in Fig. 4. Thus, one can conclude that the ring relative to the pickup coil was shifted rightwards during the recording. In practice it is not possible to align ring and coil perfectly. There will always be a slight misalignment (δ, Fig. 4A) between the center of rotation of the pickup coil and that of the ring. But this does not pose a problem for the calibration procedure, since the neuronal network will not be hampered by a misalignment. These data represent actual DMI measurements not unlike the ones that would be obtained from a human subject "wearing" a stable bite-board.

The performance of the network was assessed by a linear regression of the network's output values as function of the target values (Fig. 6B). It is apparent that the network is very well capable of fitting the data. As can be seen in the inset, the difference between network and target value, i.e. the error, varies within ±1° for different head and eye orientations. The largest errors per eye orientation occur at the most extreme head orientations (±90°) and eye orientations (±40°).

In conclusion, the network yielded an acceptable fit even with such a restricted training set and a limited number of hidden units ($N = 8$). This will be important for the application of this calibration method in subjects. In this case the dataset used for calibration has to be limited to a minimum, since time-consuming calibration measurements will considerably reduce experimental time. In addition, calibration of the entire dataset is possible demonstrating that the network can generalize the problem (data not shown).

3.2. Influence of V_{net}

We recorded the pickup/anti-coil difference signals – the difference signals for short – without the ring for the horizontal and frontal magnetic fields, as well as the primary field signals from the pickup coil and the anti-coil alone. Note here, that the secondary voltage induced by the ring (about 1 V) is 10-fold smaller than the primary field component (approximately 8–10 V peak-to-peak). Therefore, the gain of the system needs to be increased in order to obtain a sufficiently large eye orientation signal. In Fig. 7, the primary field component for the frontal (A) and the horizontal (B) field is plotted as a function of head orientation. The single coil signal (solid line) reaches a peak-to-peak amplitude of about 8 V whereas the difference signal (dashed line) reaches a peak-to-peak amplitude of about 0.5 V for the frontal and 0.2 V for the horizontal channel. The

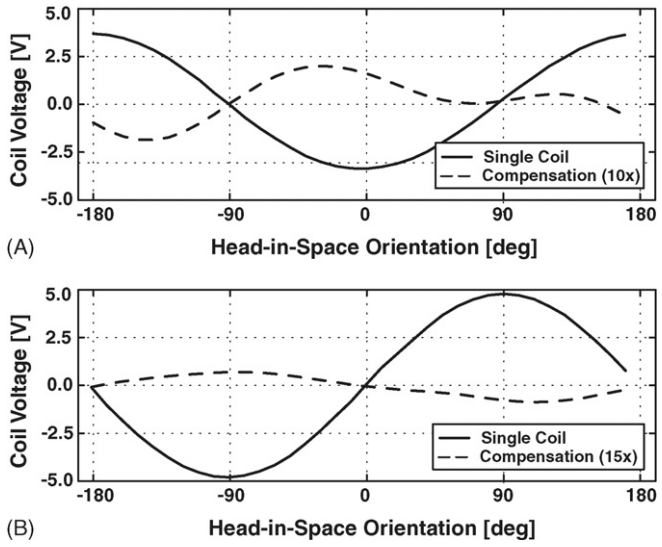

Fig. 7. Measured primary field component for a single coil (solid line) and the pickup/anti-coil compensation assembly (dashed line) for the frontal field (A) and the horizontal field (B). The gain for the single coil is 30 and 20 for the horizontal and the frontal field, respectively, and the gain for the pickup/anti-coil compensation assembly is 300 for both fields.

gain for the difference signal was thus set 10-fold higher than for the anti-coil. This amplification was also used to record the gimbal eye orientations. It is apparent that in this case V_{net} is not negligible. Thus, cancellation of the primary field is not perfect for this setup. Nevertheless, manual alignment of pickup coil and anti-coil is sufficient to ensure a secondary-to-primary component ratio such that the ring signal can be calibrated. Recording hardware saturation is avoided as well.

Note, that the resulting difference coil signals are not readily predictable. We fitted sinusoids to the pickup coil and the anti-coil signals for both the horizontal and frontal fields. The results of these fits are shown in Fig. 8A and B. Only small deviations from the data can be observed. To assess if the compensation signals for both fields can be described by the difference between two sinusoids (see Eq. (8)), we subtracted the independent signals from each other and compared them with the difference of the original two sinusoidal fits. As can be seen in Fig. 8C and D, the compensation signal cannot simply be described as the difference of two sinusoids.

4. Discussion

We have described an extension of the DMI method to record head-unrestrained gaze shifts. By including an additional perpendicular magnetic field, the inherent limited measurement range of the method (maximally 30° from straight-ahead) could be overcome. At the same time, the measurement range could be extended to the full eye-head motor range. In particular, we have shown that by using a simple, three-layer feed forward neural network with only a few hidden units, in combination with knowledge about the head orientation in space, the small ring signal can be extracted from the difference coil signal. This is even possible, when the coils are not exactly aligned, or when small inhomogeneities are present in the fields that induce a complex head position dependent offset. The neural network parameters can be determined within a minute after the calibration experiment, and can be readily used to calibrate eye movements in real time. For this to work, it is not important whether the primary field component is present in the coils or not. The obtained calibration precision with the neural network (eight hidden units) is ±1° over the entire measurement range, which is comparable to results obtained with the head-free SSC technique (Goossens and Van Opstal, 1997).

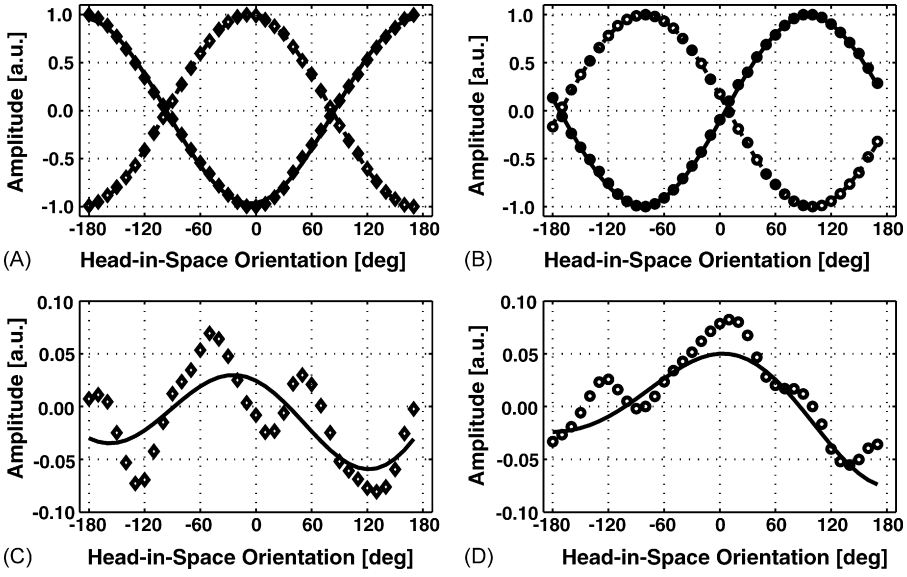

Fig. 8. Measured primary field component for the pickup coil (black symbols) and the anti-coil (open symbols) for the frontal field (A) and the horizontal field (B). The data are fitted with sinusoidal functions. (A) Pickup coil: SSE = 0.0025 and $r^2 = 0.99$ ($N = 36$); anti-coil: SSE = 0.0102 and $r^2 = 0.99$ ($N = 36$). (B) Pickup coil: SSE = 0.0307 and $r^2 = 0.99$ ($N = 36$); anti-coil: SSE = 0.0025 and $r^2 = 0.99$ ($N = 36$). Mathematical subtraction (markers) of the primary field component for the frontal (C) and horizontal (D) fields. The data are fitted with the difference of the two sinusoidal fits of the corresponding pickup coil and anti-coil.

The data presented in Fig. 6 yielded an angular resolution of about 0.3°, which is worse than the value obtainable with the SSC technique and with the head-restrained DMI method (down to 0.1°, or better). For these latter two methods, the resolution is only limited by the recording system's noise. One should bear in mind, however, that the optimal resolution of the (head-restrained) human oculomotor system is about 0.5°.

The following factors influence the resolution of the head-unrestrained DMI technique: (1) the peak-to-peak variation of the V_{net} signal, as function of head rotation, (2) the system's inherent noise, (3) the peak-to-peak variation of the ring-induced secondary signal, and (4) mechanical vibrations of the coil assembly.

It is advisable to reduce the V_{net} signal to a minimum, so that an amplification of the ring signal is possible without saturating the recording hardware at more extreme head positions. As a result, the resolution of the system increases, since the ring signal gets bigger while the noise stays the same.

Mechanical vibrations of the assembly will introduce additional low-frequency noise to the measurements that further reduce the system's resolution. These vibrations could be minimized, e.g. by having human subjects wear a bite-board on which the two coils are rigidly attached. Preliminary 2D experiments conducted with human subjects indicate a resolution of about 0.6° (recorded with a EM 7 eye movement monitor, Remmel Labs., manuscript in preparation). With experimental animals, these vibrations could be virtually eliminated by attaching the coils to head posts that are fixed to the skull.

Note here, that in experiments with head-unrestrained subjects the orientation of the head will not be known *a priori* and will have to be measured and calibrated. For example a head mounted coil could be used to measure the head movements independently. To calibrate these signals, a simple minimizing mse fitting routine could be employed (Goossens and Van Opstal, 1997) using

$$V_h^A(\gamma) = A_h \sin(\gamma + \Phi_h), \qquad V_f^A(\gamma) = A_f \cos(\gamma + \Phi_f) \quad (10)$$

with A_h, A_f, Φ_h, and Φ_f parameters. These parameters can be easily constrained. For perpendicular fields the offset angles, Φ_h and Φ_f, will be the same; the same holds true for A_h and A_f by tuning the amplifiers of the magnetic fields. This leaves only two free parameters, A and Φ, for rotations in the horizontal plane. Once these are known, the absolute head-in-space orientation, γ, can be readily extracted from the primary induction voltages in the anti-coil over the full 360° range.

A critical requirement of the extended method is a rigid fixation of the pickup coil and anti-coil to the subject's head. If not fixated rigidly, vibrations of the assembly will introduce additional low-frequency noise to the measurements. In humans, the use of a precisely fitting bite-board to which the two coils can be rigidly attached, is thus essential. In experimental animals rigid fixation can be achieved more easily by attaching both coils to the skull with bone screws and dental cement.

Our extended method is thus a promising alternative for the search coil technique. The latter one is expensive (coils may break already after a few recording sessions), while the lead wires often irritate the eye, restricting experimental time to about 40 min. The DMI method could therefore also better be suited for use on patients (provided they can use a bite-board), especially when head movements are to be incorporated (vestibular studies, blinking studies, etc.). Note also, that wire breakage is especially a problem in experimental animals. The method can also be employed for binocular recordings: as the ring's signal strength falls off rapidly with distance, the danger of interference of a ring's signal in the pickup coil of the other eye is negligible (e.g. Chaturvedi and Van Gisbergen, 2000).

In conclusion, the theory and data presented here demonstrate the feasibility of the extended DMI method for recordings in head-unrestrained subjects. The next step will be its full application in two-dimensional gaze control studies with human and non-human subjects.

Acknowledgements

We thank Stijn Martens and Hans Kleijnen for valuable technical assistance. Jeremiah Wanga is thanked for his simulations of the Biot-Savart law. This research project has been supported by a Marie Curie Early Stage Research Training Fellowship of the European Community's Sixth Framework Program under the contract number MEST-CT-2004-007825 (PB), the Neurocognition program of the Netherlands Organization for Scientific Research (NWO, project number 051.04.022 RFVDW), and the Radboud University Nijmegen (AJVO).

References

Allik J, Rauk M, Luuk A. Control and sense of eye movement behind closed eyelids. Perception 1981;10:39–51.

Bos JE, Reulen JPH, Boersma HJ, Ditters BJ. Theory of double-magnetic induction (DMI) for measuring eye movements: correction for non-linearity and simple calibration in two dimensions. IEEE Trans Biomed Eng 1988;35:733–9.

Bour LJ, Van Gisbergen JAM, Bruijns J, Ottes FP. The double-magnetic induction method for measuring eye movement—results in monkey and man. IEEE Trans Biomed Eng 1984;31:419–27.

Chaturvedi V, Van Gisbergen JA. Stimulation in the rostral pole of monkey superior colliculus: effects on vergence eye movements. Exp Brain Res 2000;132(1):72–8.

Collewijn H, Van der Mark MF, Jansen TC. Precise recordings of human eye movements. Vision Res 1975;15:447–50.

Crawford JD, Ceylan MZ, Klier EM, Guitton D. Three-dimensional eye-head coordination during gaze saccades in the primate. J Neurophysiol 1999;81:1760–82.

Goossens HHLM, Van Opstal AJ. Human eye-head coordination in two dimensions under different sensorimotor conditions. Exp Brain Res 1997;114:542–60.

Houben MM, Goumans J, Van der Steen J. Recording three-dimensional eye movements: scleral search coils versus video oculography. Invest Ophthalmol Vis Sci 2006;47:179–87.

Judge SJ, Richmond BJ, Chu FC. Implantation of magnetic search coils for measurement of eye position: an improved method. Vision Res 1979;20:535–8.

MacKay DJC. Bayesian interpolation. Neural Comput 1992;4:415–47.

Malpeli JG. Measuring eye position with the double-magnetic induction method. J Neurosci Meth 1998;86:55–61.

Remmel RS. An inexpensive eye movement monitor using the scleral search coil technique. IEEE Trans Biomed Eng 1984;31:388–90.

Reulen JPH, Bakker L. The measurement of eye movement using double-magnetic induction. IEEE Trans Biomed Eng 1982;29:740–4.

Robinson DA. A Method of measuring eye movement using a scleral search coil in a magnetic field. IEEE Trans Biomed Eng 1963;10:137–45.

Smeets JBJ, Hooge ITC. Nature of variability in saccades. J Neurophysiol 2003;90:12–20.

Van der Geest JN, Frens MA. Recording eye movements with video-oculography and scleral search coils: a direct comparison of two methods. J Neurosci Meth 2001;114:185–95.